Differential motility of p190bcr-abl- and p210bcr-abl-expressing cells: respective roles of Vav and Bcr-Abl GEFs

Thomas Daubon, Jacques Chasseriau, Ayman El Ali, Jacqueline Rivet, Alain Kitzis, Bruno Constantin, Nicolas Bourmeyster

Oncogene (2007), 1–13

www.nature.com/onc

ORIGINAL ARTICLE

Differential motility of p190$^{bcr\text{-}abl}$- and p210$^{bcr\text{-}abl}$-expressing cells: respective roles of Vav and Bcr-Abl GEFs

T Daubon[1], J Chasseriau[1], A El Ali[1], J Rivet[2], A Kitzis[1,2], B Constantin[1] and N Bourmeyster[1,2]

[1]IPBC, CNRS UMR 6187, Université de Poitiers, Poitiers, France and [2]LGCM, CHU de Poitiers, BP 577, Poitiers, France

The chimeric oncogene Bcr-Abl is known to induce autonomous motility of leukemic cells. We show here that p210$^{bcr\text{-}abl}$ responsible for chronic myelogenous leukemia induces an amoeboid type of motility while p190$^{bcr\text{-}abl}$, associated with acute lymphoid leukemia, induces a rolling type of motility. We previously reported that p210$^{bcr\text{-}abl}$ activates RhoA and Rac1, while p190$^{bcr\text{-}abl}$ although devoid of a Dbl-homology (DH) domain activates Rac1, but not RhoA. We investigated the regulation of GDP/GTP exchange factor (GEF) activities in the Bcr-Abl complex. For that purpose, different GEF activity mutants of Vav and of Bcr-Abl were constructed and stably transfected in Ba/F3 cells. Using these mutants, we demonstrate that RhoA is exclusively activated by the DH domain of p210$^{bcr\text{-}abl}$, while Rac1 activation is mostly due to Vav. Inhibition of Rac1 by Vav GEF mutant leads to immobilization of cells. Vav depletion using shRNA also induces immobilization of cells and suppression of GTP-bound Rac1. RhoA inactivation induces the specific loss of amoeboid movements. These results suggest that Rac1 activation by Vav triggers the motility of Bcr-Abl-expressing Ba/F3 cells, while the specific amoeboid mode of motility induced by p210$^{bcr\text{-}abl}$ is a consequence of RhoA activation.
Oncogene advance online publication, 3 December 2007; doi:10.1038/sj.onc.1210933

Keywords: amoeboid; Bcr-Abl; motility; Rho; Vav

Introduction

Bcr-Abl is a chimeric oncogene generated by a reciprocal translocation between chromosomes 9 and 22 (Philadelphia chromosome, Ph$^+$) that leads to the fusion of the 5′ region of the *bcr* gene with the 3′ region of the *abl* gene. This translocation is found in most patients with chronic myelogenous leukemia (CML) and a fraction of those with acute lymphoblastic leukemia (ALL) (Sawyers, 1999; Deininger *et al*., 2000). Bcr is a multidomain cytoplasmic protein composed of an oligomerization N-terminal domain, a serine kinase domain, a DH/PH domain (Dbl-Homology/Pleckstrin-homology) specific for RhoA and a C-terminal GTPase activating protein domain that inactivates Rac. Abl is a nonreceptor tyrosine kinase, which regulates among others actin reorganization, and is an important component in hematopoietic cells (Van Etten, 1999; Hernandez *et al*., 2004).

Depending on the breakpoint region of the *bcr* gene implicated in the translocation, various Bcr-Abl chimeras are observed. The most frequent one is p210$^{bcr\text{-}abl}$, which is responsible for CML (Daley *et al*., 1990), while p190$^{bcr\text{-}abl}$ is responsible for ALL (Clark *et al*., 1988). Both proteins exhibit enhanced and constitutive tyrosine kinase activity, which is the central mechanism of leukemogenesis (Lugo *et al*., 1990; Ilaria and Van Etten, 1996).

The only structural difference between these two proteins is the presence of the GDP/GTP exchange factor (GEF) domain of Bcr (Figure 1A) in p210$^{bcr\text{-}abl}$. The isolated recombinant DH domain of Bcr is an activator of Rho GTPases (Chuang *et al*., 1995). We previously reported that p210$^{bcr\text{-}abl}$ could be a GEF only for RhoA. We also identified p95^{vav} as a partner of both forms of Bcr-Abl that could be responsible for Rac1 activation (Harnois *et al*., 2003). A hypothetical model of Bcr-Abl-induced leukemogenesis involving Rho GTPases could be argued. In this model, the common activation of Rac1 and Cdc42 by p190$^{bcr\text{-}abl}$ and p210$^{bcr\text{-}abl}$ could participate in the aggressivity of Bcr-Abl-associated leukemia, by enhancing cell motility and proliferation, and by inhibiting apoptosis. In contrast, RhoA activation, specific of p210$^{bcr\text{-}abl}$-expressing cells, could be responsible for the chronic phenotype associated with this latter chimera. Some of the RhoA-induced pathways as hematopoietic differentiation should be important in this perspective (Nakashima and Nozawa, 1999).

The Vav protein family possesses three known members in mammalian cells: Vav, Vav2 and Vav3. The proto-oncogene p95^{vav} is predominantly expressed in hematopoietic cells (Bustelo, 2000). Vav is activated by tyrosine phosphorylation (Crespo *et al*., 1997) and is a substrate of Bcr-Abl (Matsuguchi *et al*., 1995). Moreover, Vav is found in complex with p210$^{bcr\text{-}abl}$ through its C-terminal SH2 domain (Bassermann *et al*., 2002). Vav has been shown to be an exchange

Correspondence: Dr N Bourmeyster, Institut de Physiologie et de Biologie Cellulaires, UMR 6187, CNRS, Université de Poitiers, 40, Avenue du Recteur Pineau, Faculte des Sciences, Pôle Biologie Santé, BP 577, Poitiers cedex 86021, France.
E-mail: n.bourmeyster@chu-poitiers.fr
Received 10 October 2006; revised 18 July 2007; accepted 2 October 2007

Table 1 Statistical analysis of time-lapse recordings of Ba/F3 cells

	Ba/F3 pGD	*Ba/F3 VAvL*	*Ba/F3 p190*	*Ba/F3 p190Vav*	*Ba/F3 p190VavL*	*Ba/F3 p190Vavt205A*	*Ba/F3 p210*	*Ba/F3 p210Vav*	*Ba/F3 p210VavL*	*Ba/F3 p210VavT205A*	*Ba/F3 p210S509A*
Percentage of cell with amoeboid movements	0	0	0	0	0	0	53 (±4)	55 (±5)	75 (±6)	29 (±4)	2 (±2)
Medium persistence time of each pseudopodia (s)	2 (±2)	7 (±5)	87 (±5)	98 (±10)	175 (±32)	52 (±8)	89 (±8)	95 (±7)	169 (±10)	47 (±5)	108 (±5)
Amount of new pseudopodia in 10 min	2 (±1)	5 (±2)	10 (±2)	15 (±6)	7 (±2)	4 (±1)	13 (±5)	15 (±2)	8 (±3)	1 (±1)	13 (±3)

Time-lapse recordings were analysed using three criteria: (1) percentage of cells showing amoeboid movements; (2) medium persistence time (s) of each pseudopodia; (3) amount of new pseudopodia appearing in 10 min. Data presented are ±s.e.m. for $n = 20$.

factor essentially for Rac1 (Crespo *et al*., 1997) and our previous results showed that Vav1 is not a GEF for RhoA (Harnois *et al*., 2003).

Rho family proteins are key regulators of cell motility. Their role has been particularly studied in mesenchymal cells (Raftopoulou and Hall, 2004). In contrast, the molecular mechanisms associated with the motility of haematopoietic cells, which are the most rapid cells, remain to be detailed. In this context, the differential activation of Rho GTPases by $p190^{bcr\text{-}abl}$ and $p210^{bcr\text{-}abl}$ should represent a useful cellular model. A characteristic of leukemic cells is to migrate outside from the haematopoietic compartment in immature states. The aim of this work was to study the Bcr-Abl-induced motility of leukemic cells and to address the role of GEF activities linked to $p190^{bcr\text{-}abl}$ or $p210^{bcr\text{-}abl}$ in this action.

Here we show that the Rac1 activation by Vav induced by Bcr-Abl leads to triggering of the motility of leukemic cells, and that the specific activation of RhoA by the DH/PH domain of $p210^{bcr\text{-}abl}$ modifies the mode of motility, which is basically a rolling type to an amoeboid type.

Results

Differential motility of Bcr-Abl-expressing Ba/F3 cells

We previously observed by confocal microscopy (Harnois *et al*., 2003) that Ba/F3p190 were spherical cells, while Ba/F3p210 cells showed stretched body with heterogeneous shapes. To question if these differential shapes corresponded to different modes of motility, we performed time-lapse recordings of cell movements in 3D matrigel or collagen. The only morphological change between wild-type Ba/F3 and empty vector-expressing cells (Ba/F3pGD) was a slight volume increase. Both cell types presented no cellular movements and remained spherical, smooth and immobile during the recording time (Figure 1Ba,b). Ba/F3p190 cells remained strictly spherical during recording, while Ba/F3p210 cells showed characteristic amoeboid movements (Figure 1Bc,d). Ba/F3p190 cells were highly mobile cells using a rolling-type motility, crawling into 3D matrigel with the help of pseudopodia. In contrast, Ba/F3p210 cells showed spontaneous cell motility by amoeboid movements. During 10 min recording, we observed that 53% of Ba/F3p210 cells displayed amoeboid cell motility (Table 1). However longer observations indicated that all Ba/F3p210 cells were able to be spontaneously mobile but not synchronously. All cells cycled between resting periods in which the cell body was either spherical or irregular, and mobile periods with changes in cell body shape characteristic of amoeboid movements.

In transwell experiments through 3D matrigel, wild-type Ba/F3 and Ba/F3pGD cells presented no spontaneous motility. In contrast, Ba/F3p190 and Ba/F3p210 cells spontaneously colonized and moved into 3D matrigel. The migration rate of Ba/F3p190 cells was significantly higher than Ba/F3p210 cells (Figure 1C).

ShRNA inhibition of Vav expression leads to cell immobilization

We previously showed that Rac1 was activated in both Ba/F3p190 and Ba/F3p210 cells, while RhoA was found in an activated state only in Ba/F3p210 cells (Harnois *et al*., 2003). We also demonstrated the presence of active $p95^{vav}$ in Bcr-Abl complexes. In order to understand the role of Vav in Bcr-Abl-induced cell motility, we transfected shRNAs to deplete Vav in Ba/F3pGD, Ba/F3p190 and Ba/F3p210 cells. An 85% inhibition of Vav expression was obtained using shRNA1 as assessed by fluorescence-activated cell sorting (FACS) analysis (data not shown) or western blot analysis (Figure 2a). The amount of activated Rac1 was significantly lowered in shRNA1-transfected cells in comparison with control-shRNA- or shRNA2-transfected cells, except in Ba/F3pGD in which it remained constantly low (Figure 2a). Transwell analysis of cell migration through 3D matrigel indicated that control-shRNA or shRNA2 induced no modification of cell motility. In contrast, transfection of shRNA1 led to a dramatic inhibition of Ba/F3p190 and Ba/F3p210 cell motility, while Ba/F3pGD cells remained immobile (Figure 2b).

Expression and characterization of Vav and Bcr-Abl mutants in Ba/F3 cells

To address the specificity of GEF activities in different Bcr-Abl complexes and consequently the role of Rho GTPases in the motility processes, we constructed and expressed mutants of the GEFs previously found associated with Bcr-Abl (Harnois *et al*., 2003). Previous reports used deletion mutants of Vav, containing only its C-terminal SH3 and SH2 domains (Bassermann *et al*., 2002). These constructs act as dominant-negative mutants of Vav for all of its activities. As well as Vav knockdown, they did not address the specific question of GEF activity. We then constructed a point mutant in the DH domain (VavT205A) similar to the one described for Dbl and SoS (Zheng *et al*., 1997) (Figure 3a). We established stable cell lines expressing Vav (Vav, VavL and VavT205A) tagged at their N terminus with poly-His in Ba/F3 cells or in previously selected Ba/F3 lines expressing $p190^{bcr\text{-}abl}$ or $p210^{bcr\text{-}abl}$. The expression of Vav constructs was assessed by pHis and Vav immunoblots (Figure 3b and Supplementary data, Figure 1).

Selection of Ba/F3p210S509A cells was performed as previously described (Daley and Baltimore, 1988), independence toward interleukin-3 (IL-3) was obtained after 1 week of culture. Western blot of anti-Abl immunoprecipitation in Ba/F3p190, Ba/F3p210 and Ba/F3p210S509A cells revealed by anti-Abl antibody showed that the expression levels of $p190^{bcr\text{-}abl}$, $p210^{bcr\text{-}abl}$ and $p210^{bcr\text{-}abl}$S509A were equivalent (Figure 3c). No difference in Bcr-Abl-induced tyrosine phosphorylation was observed as assessed by PY-20 labeling of Ba/F3p190, Ba/F3p210 and Ba/F3p210S509A cell lysates. These phosphorylations were specifically inhibited by CGP-571 (Novartis, Switzerland) in each Bcr-Abl-expressing cells (Figure 3d). Vav was found in complex with every form of Bcr-Abl, as assessed by immunoprecipitations using anti-Vav or anti-Abl antibodies (Figure 3e). As compared to $p190^{bcr\text{-}abl}$ or $p210^{bcr\text{-}abl}$, the cellular localization of $p210^{bcr\text{-}abl}$S509A was totally similar, in the actin cortex (Supplementary data, Figure 2).

The GEF domain of Vav is responsible for Rac1 activation, while RhoA activation is specifically due to the GEF domain of $p210^{bcr\text{-}abl}$

To measure the activation state of Rac1 or RhoA in different cell lines, we performed pull-down assays. Expression of Vav in Ba/F3p190 or Ba/F3p210 cells induced no change in Rac1 activation state. Expression of VavL in wild-type Ba/F3 cells induced the enhancement of activated Rac1 level, but not of RhoA (Figures 4a and b). Expression of VavL enhanced by approximately twofold the activation state of Rac1 in Ba/F3p190VavL and Ba/F3p210VavL cells in comparison with Ba/F3p190 and Ba/F3p210 cells. In contrast, expression of VavT205A greatly lowered the level of activated Rac1 in Ba/F3p190VavT205A and Ba/F3p210VavT205A cells (Figure 4a). The inhibitory effect of VavT205A and the enhancing effect of VavL clearly indicate that the GEF domain of Vav is responsible for Rac1 activation induced by $p190^{bcr\text{-}abl}$ and $p210^{bcr\text{-}abl}$. We also measured the activation state of RhoA in Ba/F3p210S509A cells in comparison with Ba/F3p190 and Ba/F3p210 cells. As observed in Ba/F3p190 cells, no active RhoA was found in Ba/F3p210S509A cells in contrast to Ba/F3p210 cells (Figure 4b).

Taken together, these results demonstrated that (1) VavT205A and $p210^{bcr\text{-}abl}$S509A mutants have no GEF activity, (2) Vav is the major activator of Rac1 in Ba/F3p190 and Ba/F3p210 cells and (3) $p210^{bcr\text{-}abl}$ is the unique vector of RhoA activation in Ba/F3p210 cells.

Vav and Bcr-Abl modulate the motility of Ba/F3 cells

The role of Rho GTPases in cell motility has been well documented (Raftopoulou and Hall, 2004). We analysed cell movements by time-lapse microscopy recording in 3D matrigel and studied the spontaneous migration of the cell lines through 3D matrigel using transwell experiments.

In time-lapse recordings, co-expression of Vav in Ba/F3p190 or Ba/F3p210 cells induced no modification of motility, pseudopodia production or velocity in comparison with Ba/F3p190 and Ba/F3p210 cells (Figures 1Ac, d, 5b and e and Table 1). Co-expression of VavL in Ba/F3p190 or Ba/F3p210 cells greatly enhanced the proportion of spontaneously mobile cells observed during 10 min (Figures 5c and f). Interestingly, expression of VavL in wild-type Ba/F3 cells induced no significant change in pseudopodia production, and no motile cell was observable (Figure 5a and Table 1). In contrast, co-expression of VavT205A in Ba/F3p190 or Ba/F3p210 cells totally inhibited cell motility (Figures 5d and g). Conversely, Ba/F3p210S509A cells are highly mobile cells (Figure 5h). The velocity of Ba/F3p190, Ba/F3p190Vav, Ba/F3p190VavL, Ba/F3p210, Ba/F3p210Vav, Ba/F3p210VavL and Ba/F3p210S509A cells was comparable, and comprised between 200 and 800 nm h^{-1}.

Both Ba/F3p190 and Ba/F3p210 cells produced short and active pseudopodia, which could be qualified as ruffles, filopodia and occasionally lamellipodia. The production and the persistence of these pseudopodia were comparable between Ba/F3p190, Ba/F3p190Vav Ba/F3p210 and Ba/F3p210Vav cells (Table 1). Expression of VavL in Ba/F3p190 or Ba/F3p210 cells led to similar results: enhancement of the persistence of pseudopodia, which were longer and larger, and a 50% inhibition of pseudopodia production (Table 1). In contrast, VavT205A expression almost abolished the production of new pseudopodia, which were less persistent, short and diffuse along the membrane (Figures 5d and g and Table 1).

Co-expression of VavL in Ba/F3p210 cells enhanced the proportion of cells showing amoeboid movements. In 29% of Ba/F3p210VavT205A cells, we observed inefficient cell body deformation similar to amoeboid movements. Interestingly, amoeboid deformation of Ba/F3p210VavT205A cell bodies was slowed down in comparison with Ba/F3p210 and Ba/F3p210VavL cells (movie 3 in Supplementary data). An inefficient

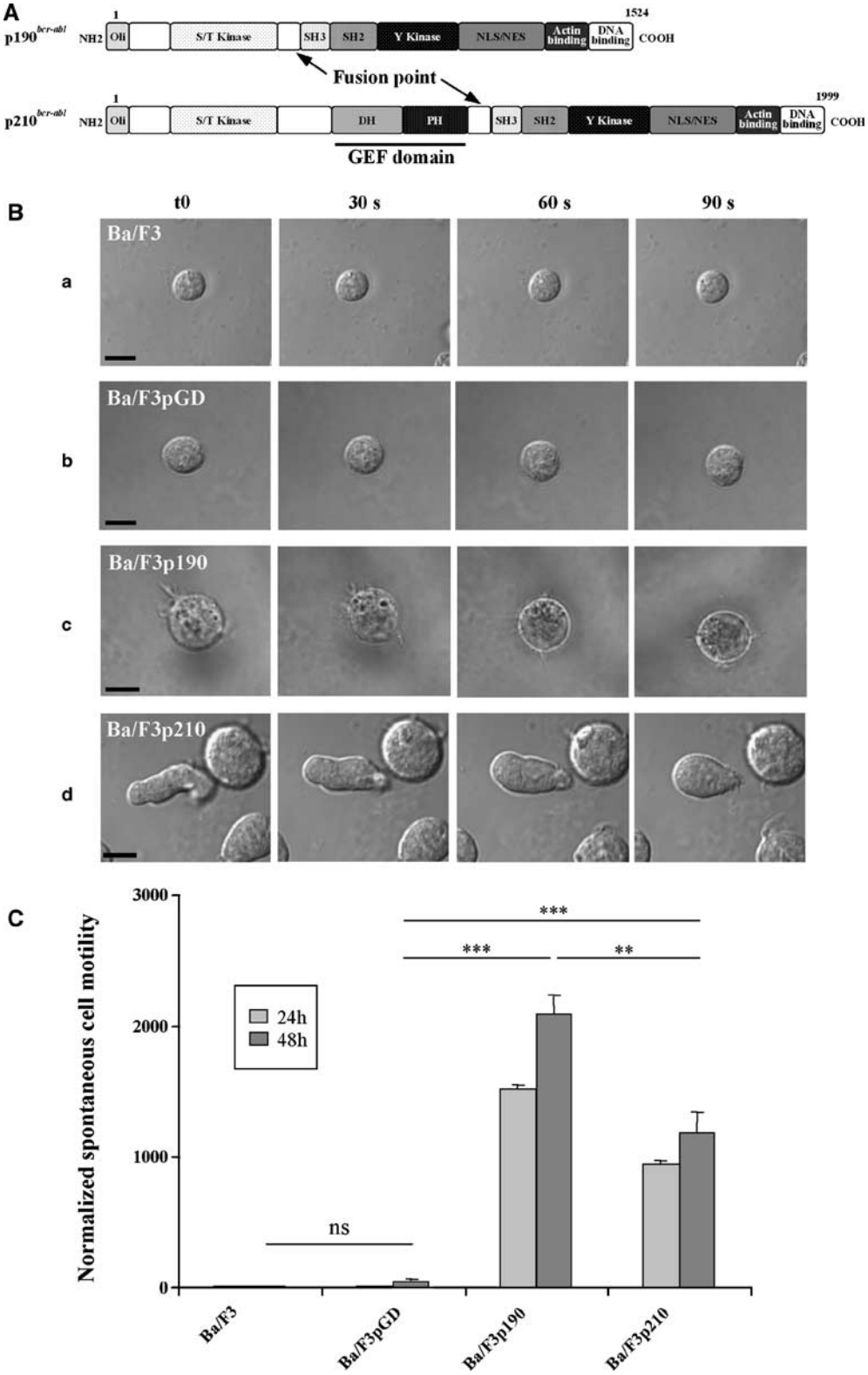

Figure 1 Differential motility of Ba/F3p190 and Ba/F3p210 cells in 3D matrigel. (**A**) Domain structure of the different Bcr-Abl chimera. (**B**) Time-lapse recording of wild-type Ba/F3, Ba/F3pGD, Ba/F3p190 and Ba/F3p210 cell movements in 3D matrigel. Images were extracted from time-lapse recording every 30 s for 90 s. Full-length recordings (300 s, one image per s) are visible in Supplementary Material (movie 1). Scale bar: 10 μm. (**C**) Transwell measurement of Ba/F3, Ba/F3p190 and Ba/F3p210 cell motility. A total of 2.5×10^4 cells of each type were added in 3D matrigel coated on 8 μm porous filters inserts. Both compartments contained the same RPMI 1640 complete medium. Cell counting was performed 24 and 48 h after seeding. Raw data of each cell type are divided by the specific proliferation rate measured in parallel, then normalized to wild-type Ba/F3 cells. Results shown are mean values ± s.d. ($n = 5$). Unpaired Student's *t*-test was used for statistical analysis. $^{**}P < 0.01$, $^{***}P < 0.001$; ns, nonsignificant.

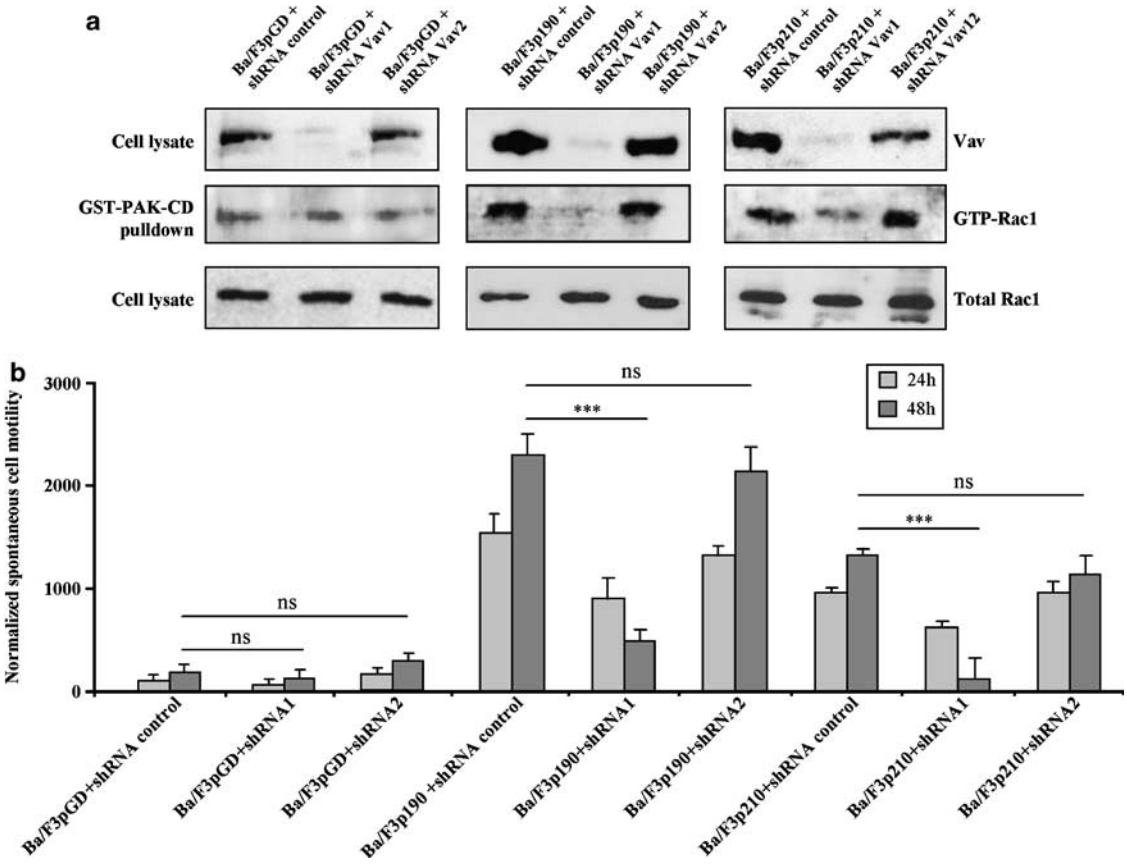

Figure 2 Vav-depleted cells contain no activated Rac1 and loose motility. (**a**) Characterization of shRNA-induced depletion of Vav. Ba/F3pGD, Ba/F3p190 and Ba/F3p210 cells (2×10^6) were transfected with 2 μg of plasmids containing (1) a control shRNA sequence and (2) *vav*-specific shRNA sequences (shRNA1 and shRNA2) using a Nucleofector device (Amaxa). After 48 h of culture, cells were lysed as described in the 'Material and methods' section, and 20 μg of total protein was loaded on an 11% SDS–PAGE, western blotted and revealed using anti-Vav or anti-Rac1 antibodies (upper and lower panels). In parallel, pull-down assay was performed on 200 μg of protein using GST-PAK-CD as a bait for GTP-bound Rac1. Bead-bound proteins were loaded onto 13% SDS–PAGE, western blotted and revealed using anti-Rac1 antibody (middle panel). (**b**) Transwell measurement of shRNA-transfected cells. Results were obtained as in Figure 1C and are mean values ± s.d. ($n = 3$).

amoeboid deformation was also observed in a minority of Ba/F3p210S509A cells (Table 1). A rolling-type motility using pseudopodia without deformation of the cell body, similar to Ba/F3p190 cells was observed for more than 90% of Ba/F3p210S509A mobile cells.

The spontaneous motility of Ba/F3 cells was studied in transwell experiments through 3D matrigel. Expression of Vav had no effect on the invasion of Ba/F3p190 or Ba/F3p210 cells (Figure 6a). In contrast, expression of VavL in Ba/F3p190 or in Ba/F3p210 cells induced a 4- to 4.5-fold enhancement of cell motility, while in wild-type Ba/F3 cells no significant enhancement of motility was observed. Conversely, expression of VavT205A in Ba/F3p190 or in Ba/F3p210 cells inhibited cell motility to a level nearly comparable to wild-type Ba/F3 or Ba/F3pGD cells. Ba/F3p210S509A cells presented a 2.5-fold enhancement of migration rate in comparison with Ba/F3p210 cells (Figure 6a).

Amoeboid movements are the consequence of p210$^{bcr\text{-}abl}$-induced RhoA activation

C3 exoenzyme from *Clostridium botulinum* is an adenosine diphosphate-ribosyl transferase that specifically inhibits RhoA, although it is active on RhoB and RhoC as well. To address the role of RhoA in cell motility, we treated Ba/F3 strains with C3 for 6 h.

In transwell experiments through 3D matrigel, C3 exoenzyme treatment induced no modification in the motility of Ba/F3p190 cells, co-expressing or not Vav or Vav mutants. In contrast, an enhancement of spontaneous motility of Ba/F3p210 cells expressing or not Vav or Vav mutants was observed (Figure 6b). It is noticeable that C3-treated Ba/F3p210 cells exhibited an enhancement of spontaneous motility to a level comparable to Ba/F3p210S509A cells. Interestingly, motility of Ba/F3p210S509A cells was not affected by C3 exoenzyme treatment.

In time-lapse recordings of cell movements, Ba/F3p190 cells, co-expressing or not Vav or Vav mutants, exhibited no change after C3 treatment, even after 24 h (Figures 7c–f). In contrast, Ba/F3p210, Ba/F3p210Vav, Ba/F3p210VavL and Ba/F3p210VavT205A cells were subjected to strong modifications (Figures 7g–j). The amoeboid cell body shape characteristic of p210$^{bcr\text{-}abl}$-expressing cells was lost, changed into a spherical shape comparable to p190$^{bcr\text{-}abl}$-expressing cells. No modification of Ba/F3p210S509A cell shape was observed after

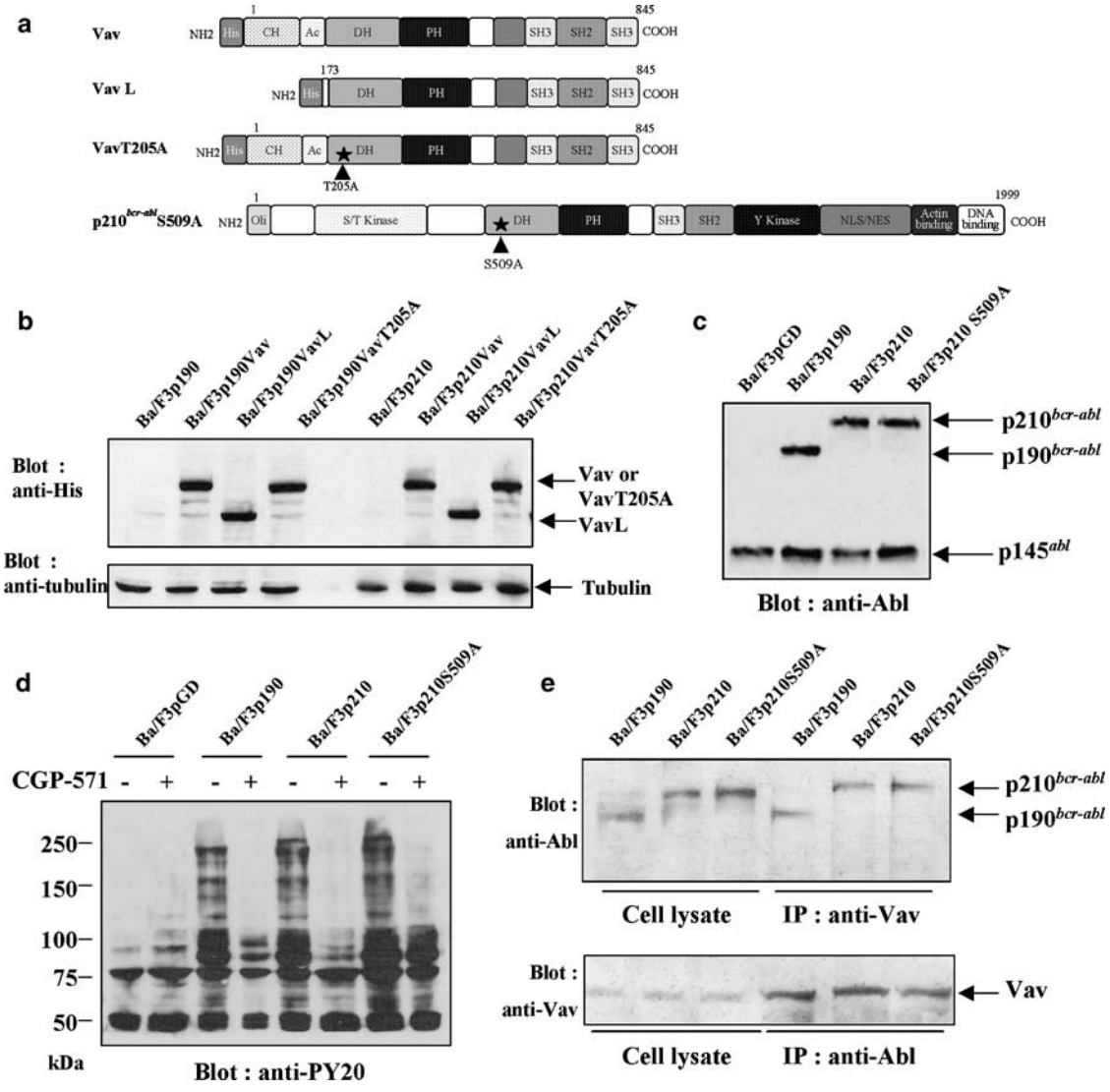

Figure 3 Characterization of mutant-GEF-expressing cells. (**a**) Domain structure of Vav, VavL and p210$^{bcr\text{-}abl}$ showing the position of VavT205A and p210$^{bcr\text{-}abl}$S509A point mutations. (**b**) Expression of Vav and Vav mutants in Ba/F3 cells. A total of 5×10^5 cells of each type were lysed in Laëmmli loading buffer and migrated in 9% SDS–PAGE and blotted onto nitrocellulose membrane. pHis-tagged proteins were visualized using anti-His antibody. In parallel, 1/10 of the lysates were loaded onto a 10% SDS–PAGE, blotted and revealed using anti-tubulin antibody to assess of the total protein loading. (**c**) Expression of Bcr-Abl chimera in Ba/F3 cells: 20 μg of Ba/F3pGD, Ba/F3p190, Ba/F3p210 and Ba/F3p210S509A cell lysates were loaded onto an 8% SDS–PAGE and immunoblotted using anti-Abl antibody. (**d**) Tyrosine-kinase activity of Bcr-Abl chimera expressed in Ba/F3 cells. A total of 2×10^5 Ba/F3pGD, Ba/F3p190, Ba/F3p210 and Ba/F3p210S509A cells were seeded in 24-well plate and incubated in RPMI 1640 complete medium containing or not 10 μM CGP-571 for 12 h. Cells were then lysed in lysis buffer containing 100 μM vanadate and 10 μg of total protein was loaded onto a 9% SDS–PAGE. The western blot was revealed using PY-20 antibody. (**e**) Presence of Vav in complex with each Bcr-Abl chimera. Ba/F3p190, Ba/F3p210 and Ba/F3p210S509A cells were lysed as described in the 'Materials and methods' section. Lysates (200 μg) were incubated with anti-Vav (upper panel) or anti-Abl (lower panel) antibody and immunoprecipitation was performed as described in the 'Materials and methods' section. Lysates (10 μg) and immunoprecipitates migrated onto 8% SDS–PAGE were then blotted on nitrocellulose membrane. The presence of Bcr-Abl chimera or Vav were revealed using anti-Abl antibody (upper panel) or anti-Vav antibody (lower panel).

C3 treatment (Figure 7k). Pseudopodia protrusion, length and persistence were not affected by C3 exoenzyme treatment in any cell type (Table 2).

Discussion

Cell motility has been extensively studied for the last 15 years, but almost exclusively for the mesenchymal mode of motility and on 2D surfaces. Haematopoietic cells, which are the most rapid cells, move quite differently (Friedl and Wolf, 2003). We show here that, as many other haematopoietic cells, Ba/F3p210 cells use an amoeboid mode of motility. In contrast, Ba/F3p190 cells, while highly motile, show no amoeboid motility and crawl by rolling. In a previous report, we have shown that the major difference between these chimeras resides in p210$^{bcr\text{-}abl}$ ability to activate RhoA (Harnois *et al*., 2003). While the macromolecular complexes

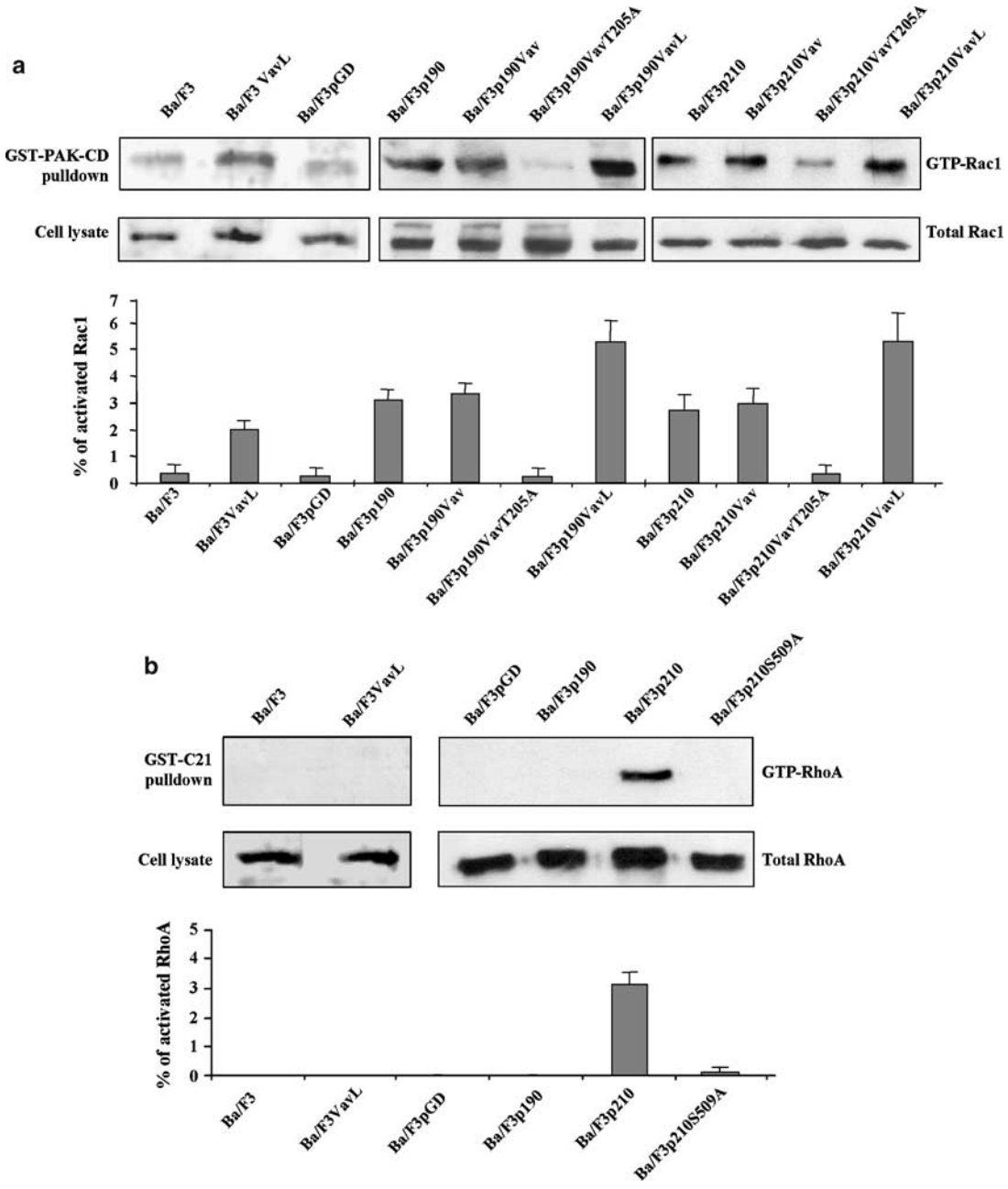

Figure 4 The GEF activities of Vav and p210$^{bcr\text{-}abl}$ are specific for Rac1 and RhoA, respectively. (**a**) The activation state of Rac1 in Ba/F3 cells. Cells were lysed as described in the 'Materials and methods' section. Lysates (200 μg) were incubated with 10 μg of sepharose-bound GST-fused PAK-CD. Bead-bound complexes comprising activated (GTP-bound) form of Rac1 were revealed by western blot using anti-Rac1 antibody. For comparison, the relative amount of Rac1 present in 20 μg of total lysate from each cell line is shown. Results are representative of five independent experiments. Graph (lower panel) shows the percentage of activated GTPase in each cell type measured after densitometric analysis by Scion Image of bands revealed by anti-Rac1 antibody ± s.d. ($n = 5$). (**b**) The activation state of RhoA in Ba/F3 cells. Parental Ba/F3, Ba/F3VavL, Ba/F3pGD, Ba/F3p190, Ba/F3p210 and Ba/F3p210S509A cells were lysed as described in the 'Materials and methods' section. The experiment was performed as in (**a**) using GST-fused RBD of Rhotekin-C21 and anti RhoA antibody ($n = 5$).

organized around p190$^{bcr\text{-}abl}$ or p210$^{bcr\text{-}abl}$ presented a GEF activity toward Rac1 and Cdc42, the macromolecular complex organized around p210$^{bcr\text{-}abl}$ was the only one able to activate RhoA. It has been shown that Bcr-Abl enhances the motility of leukemic cells, through actin cytoskeletal proteins phosphorylation and abnormal integrin function (Salgia *et al*., 1997; Bhatia *et al*., 1999). However, the role of Rho-GTPases and Bcr-Abl-associated GEF activities in these changes has never been explored. The tyrosine-kinase-independence of adhesion abnormalities induced by Bcr-Abl (Wertheim *et al*., 2002), and the comparable tyrosine-kinase activities of p190$^{bcr\text{-}abl}$ and p210$^{bcr\text{-}abl}$ (Ilaria and Van Etten, 1996; Figure 2d) suggest that differential cell

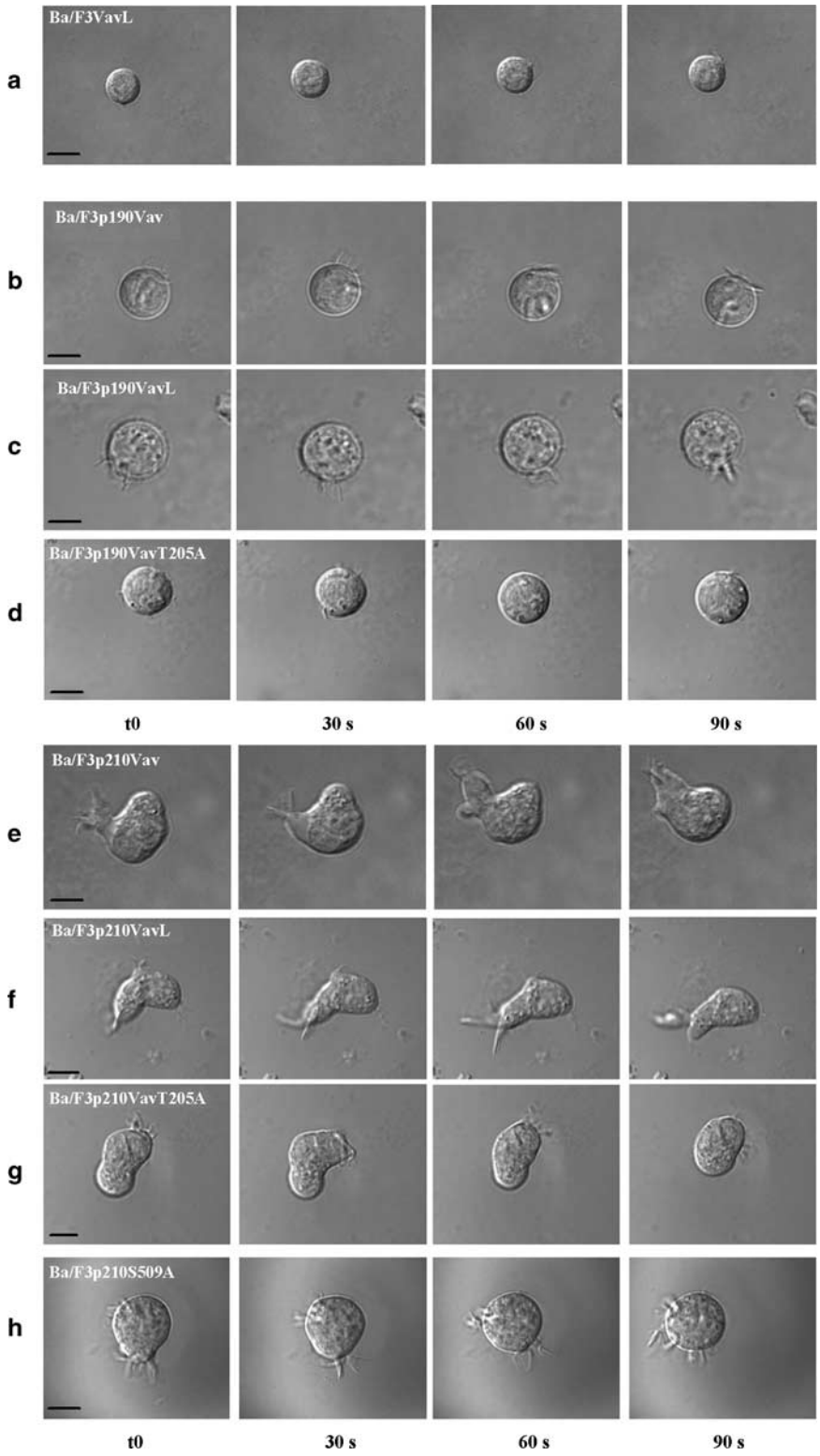

Figure 5 GEF-domain mutations of Vav and $p210^{bcr\text{-}abl}$ lead to dramatic modifications of Ba/F3 cell movements in 3D matrigel. Images were extracted from time-lapse recording every 30 s for 90 s. Full-length recordings (300 s, one image per s) are visible in Supplementary Materials (movies 2 and 3). Figure shows the time-lapse recordings of Ba/F3VavL (**a**), Ba/F3p190Vav (**b**), Ba/F3p190VavL (**c**), Ba/F3p190VavT205A (**d**), Ba/F3p210Vav (**e**), Ba/F3p210VavL (**f**), Ba/F3p210VavT205A (**g**) and Ba/F3p210S509A (**h**) cells. Scale bar: 10 μm.

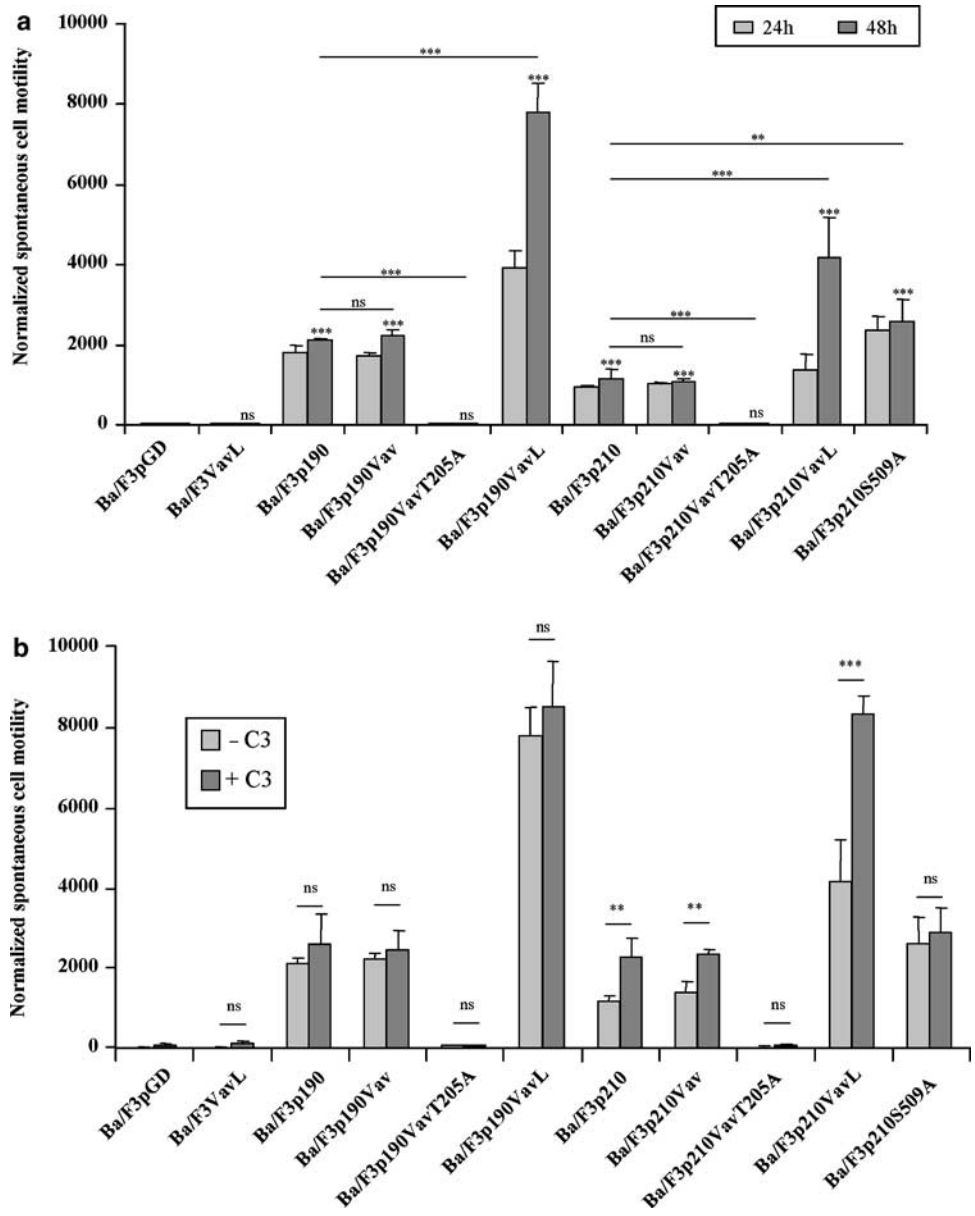

Figure 6 (**a** and **b**) GEF-domain mutations of Vav and $p210^{bcr\text{-}abl}$ induce important changes in Ba/F3 cell motility through 3D matrigel. A total of 2.5×10^4 cells of each type were added in 3D matrigel coated on 8 μm porous filters inserts. Both compartments contained the same RPMI 1640 complete medium. In the lower panel (**b**), cells were pretreated by C3 for 6 h before seeding. Results were obtained as in Figure 1C and are mean values ± s.d. ($n = 4$). Asterisks over the 48 h bars of each cell types represent the *P*-values calculated in comparison with Ba/F3pGD cell motility.

movements are not related to tyrosine-kinase activity. Our previously published data argued for a role of Vav in Bcr-Abl-associated complexes toward Rac1 and of the DH/PH domain of $p210^{bcr\text{-}abl}$ toward RhoA although no data existed to attribute the GEF activity to one of the known components of the complex.

We first depleted the Bcr-Abl-expressing cells of Vav using shRNA. Interestingly, in addition to the loss of activated Rac1, already observed with dominant-negative Vav (Bassermann *et al*., 2002), a dramatic decrease in spontaneous motility through 3D matrigel was obtained as assessed by transwell experiments (Figure 2b). To address the respective role of Rho GTPases in the motility processes, we constructed and expressed negative mutants of the GEFs previously found associated with Bcr-Abl (Harnois *et al*., 2003). The VavT205A mutant, different from previously used deletion mutants (Bassermann *et al*., 2002), was designed to address the specific question of GEF activity. Interestingly, Vav-depleted Ba/F3p210 cells still presented amoeboid shape in time-lapse experiments (data not shown). From our *in vitro* experiments and cellular behavior observations, we can conclude that the T205A mutant is devoid of GEF activity toward Rac1. Indeed, in Ba/F3p210VavT205A and Ba/F3p190VavT205A cells only residual activated Rac1 was observed,

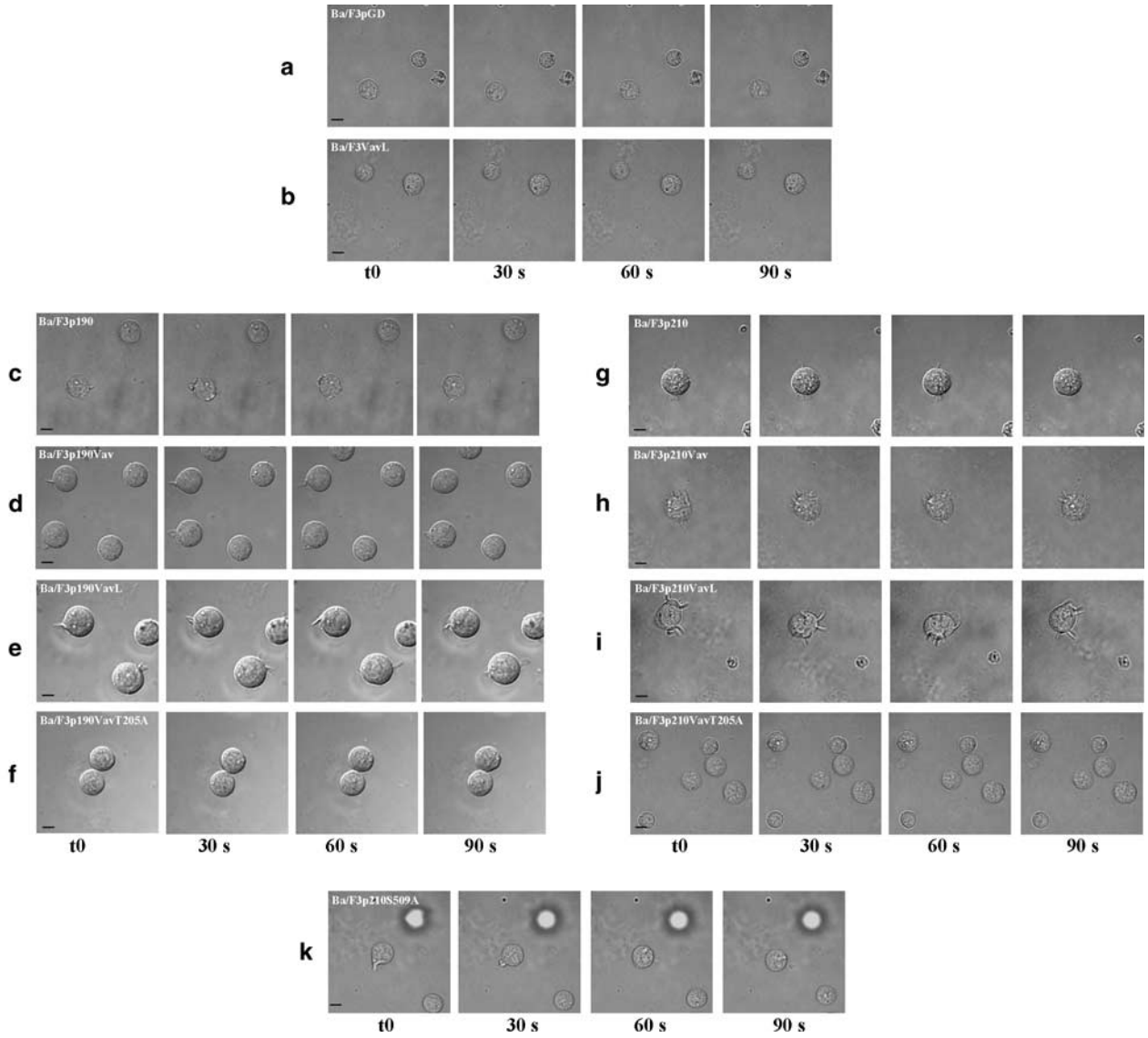

Figure 7 C3 exoenzyme specifically inhibits the amoeboid movements of Ba/F3p210 cells. Images were extracted from time-lapse recording every 30 s for 90 s. Full-length recordings (300 s, one image per s) are visible in Supplementary Materials (movies 4 and 5). Figure shows the time-lapse recordings of Ba/F3pGD (**a**), Ba/F3VavL (**b**), Ba/F3p190 (**c**), Ba/F3p190Vav (**d**), Ba/F3p190VavL (**e**), Ba/F3p190VavT205A (**f**), Ba/F3p210 (**g**), Ba/F3p210Vav (**h**), Ba/F3p210VavL (**i**), Ba/F3p210VavT205A (**j**) and Ba/F3p210S509A (**k**) cells. Scale bar: 10 μm.

comparable to the level in wild-type Ba/F3 cells (Figure 4a). *In vitro* GEF activity measurements of purified VavT205A showed no activity toward Rac1 (data not shown), while purified Vav from Ba/F3p190 or Ba/F3p210 cells presented a classical GEF activity toward Rac1 (Harnois *et al*., 2003).

The present results clearly show that the DH/PH domain of $p210^{bcr\text{-}abl}$ is uniquely responsible for RhoA activation in $p210^{bcr\text{-}abl}$-expressing cells, which in turn leads to amoeboid movements. Indeed, expression of the $p210^{bcr\text{-}abl}$S509A mutant totally abolished the presence of GTP-bound RhoA. We show here that the S509A mutation on $p210^{bcr\text{-}abl}$ suppresses RhoA activation and amoeboid-type motility of Ba/F3 cells (Figures 4b and 5h). Similarly, C3-exoenzyme treatment of $p210^{bcr\text{-}abl}$-expressing cells suppressed the presence of amoeboid movements (Figures 7g–j). We can conclude that the DH domain of $p210^{bcr\text{-}abl}$ is the unique vector of RhoA activation in this model, and that RhoA activation is responsible for the amoeboid mode of motility, as observed in several models (Yamazaki *et al*., 2005).

Our results show that Vav is the major GEF responsible for Rac1 activation. Inhibition of the GEF activity of Vav and consequently inactivation of Rac1 induced the loss of membrane protrusion production and ruffles, but also abolished the motility of $p190^{bcr\text{-}abl}$- and $p210^{bcr\text{-}abl}$-expressing cells (Figures 5 and 6). Conversely, constitutive activation of Vav induced a spectacular enhancement of migration rate

Table 2 Statistical analysis of time-lapse recordings of C3 exoenzyme-treated Ba/F3 cells

	Ba/F3 pGD	*Ba/F3 VavL*	*Ba/F3 p190*	*Ba/F3 p190Vav*	*Ba/F3 p190VavL*	*Ba/F3 p190 VavT205A*	*Ba/F3 p210*	*Ba/F3 p210Vav*	*Ba/F3 p210VavL*	*Ba/F3 p210VavT205A*	*Ba/F3 p210S509A*
Percentage of cells with amoeboid movements	0	0	0	0	0	0	0	0	0	0	2 (±1)
Medium persistence time of each pseudopodia (s)	3 (±2)	2 (±2)	72 (±15)	90 (±10)	176 (±12)	61 (±8)	99 (±8)	95 (±7)	149 (±20)	96 (±5)	102 (±8)
Amount of new pseudopodia in 10 min	5 (±2)	6 (±2)	13 (±3)	15 (±5)	9 (±2)	1 (±1)	13 (±5)	14 (±2)	9 (±3)	2 (±1)	16 (±5)

Ba/F3 cells were treated as described in the 'Materials and methods' section. Time-lapse recordings were analysed using three criteria: (1) percentage of cells showing amoeboid movements; (2) medium persistence time (s) of each pseudopodia; (3) amount of new pseudopodia appearing in 10 min. Data presented are ± s.e.m. for $n = 15$.

of Bcr-Abl-expressing cells, but no modification of the mode of motility (that is, rolling for $p190^{bcr\text{-}abl}$ versus amoeboid for $p210^{bcr\text{-}abl}$). Noticeably, C3-exoenzyme treatment, which did not affected the spontaneous motility of $p190^{bcr\text{-}abl}$-expressing cells in transwell experiments, conversely enhanced $p210^{bcr\text{-}abl}$-expressing cell migration. C3 treatment was known to totally inhibit the spontaneous motility of bovine neutrophils (Stasia *et al*., 1991). Thus, the presence of spontaneous motility in absence of RhoA activation could be a specificity of Bcr-Abl. We can then conclude that the GEF activity of Vav is indispensable for Bcr-Abl-induced motility, while RhoA activation by the DH domain of $p210^{bcr\text{-}abl}$ do not trigger motility but promotes an amoeboid type. Activation of RhoA and thus the presence of amoeboid movements may slow down the spontaneous motility of Bcr-Abl-expressing cells. Recently, Rho pathway was identified as a target for Bcr-Abl, but inhibition of RhoA induced a decrease in SDF-1-stimulated motility (Unwin *et al*., 2005). It should be noted that we studied the spontaneous motility of Bcr-Abl-expressing cells, and not the chemokine-induced motility.

Our data demonstrates a key role of Vav in cooperation with Bcr-Abl in the induction of leukemic cell motility. The Bcr-Abl-expressing cells also represent a useful model to study the role of Rho GTPases in the motility of nonmesenchymal cells which is actually poorly understood. The comprehension of the molecular mechanisms of cytoskeleton remodeling leading to amoeboid movements or to rolling would give new insights in the cell biology of motility. In this cellular model (Figure 8), the major activation of Vav and Rac1 by Bcr-Abl stimulates the migration of leukemic cells by a rolling type, which seems to be the basic mode of motility of Bcr-Abl-expressing cells. When the $p210^{bcr\text{-}abl}$ chimera is expressed, the specific activation of RhoA by the DH/PH domain leads to the transition to an amoeboid mode of motility.

Future work on patient cells should help to explore the consequences for leukemic cells of the changes in motility mode and to determine if the $p210^{bcr\text{-}abl}$-induced amoeboid mode of motility is related to the chronic phenotype, while the rolling mode of motility is in relation with the more aggressive phenotype linked to $p190^{bcr\text{-}abl}$.

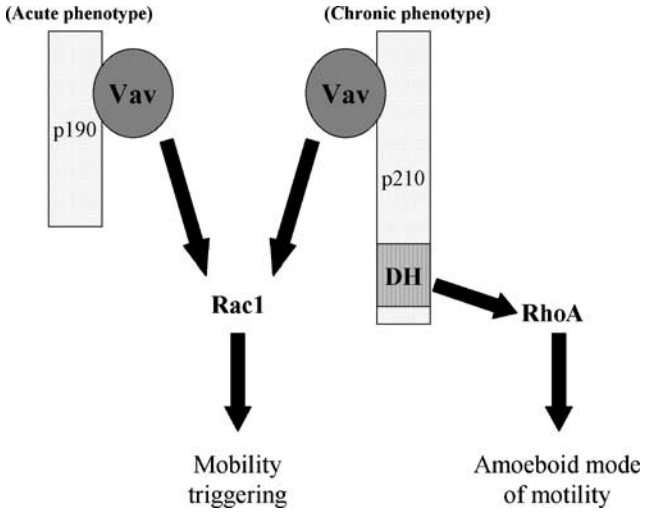

Figure 8 Hypothetical model describing the Rac1- and RhoA-induced modes of motility as activated by $p190^{bcr\text{-}abl}$ or $p210^{bcr\text{-}abl}$.

Materials and methods

Cell lines and cDNA constructs

Culture of Ba/F3 and Bcr-Abl-expressing cell lines Ba/F3p210 and Ba/F3p190 was described previously (Harnois *et al*., 2003). The pGD210S509A vector was obtained by directed mutagenesis of pGD210 vector using the QuickChange kit (Stratagene, France) with specific primer. Ba/F3p210S509A cell line was obtained as described for Ba/F3p210 and Ba/F3p190 cells (Daley and Baltimore, 1988) and grew in the absence of IL-3. A Ba/F3 cell line expressing the pGD empty vector (Ba/F3pGD) was obtained, and grew in the presence of G418 (0.7 mg ml^{-1}) and rm-IL-3 (10 ng ml^{-1}).

Vav cDNA was cloned in the expression vector pEF4A/His (Invitrogen, Cerey-Pontoise, France) between EcoRI and XbaI sites. VavT205A mutation was obtained using the QuickChange mutagenesis kit (Stratagene) using specific primer. Truncated cDNA of vavL was generated by creating an EcoRI

site at codon 171 of the cDNA of wt Vav cloned in EF4A/His (Invitrogen) followed by digestion using EcoRI. Every cDNAs were subjected to sequence analysis to avoid the possibility of additional mutations.

To obtain Vav- or mutant-Vav-expressing cells, Ba/F3p190 and Ba/F3p210 cells were co-transfected by electroporation with pEF4A vector containing the cDNAs of the different forms of Vav. After 2 days of transfection, selection was applied by adding use zeocin (0.04% w/v) for 3 weeks. Cloning of cell lines was made by selection in 96 wells of dilutions to 0.3 cell per well. Cells were then cultured in the presence of zeocin (0.04% w/v) and survived without IL-3 except Ba/F3VavL cells, which remained dependent on rm-IL-3 ($10\,ng\,ml^{-1}$).

Antibodies

Antibodies used were anti-Abl mouse monoclonal antibody 8E9 (Becton-Dickinson, Pont de Claix, France), anti-polyHis mouse monoclonal (Clontech, Ozyme, St-Quentin-en-Yvelines, France), anti-RhoA (26C4, mouse monoclonal, Santa Cruz Biotechnology, Tebu Bio Le Perray en Yvelyne, France), anti-Rac (mouse monoclonal 23A8, Upstate Biotechnology, Euromedex, Souffelweyersheim, France), anti-Vav (mouse monoclonal, Upstate Biotechnology), anti-Vav (H-111 rabbit polyclonal, Santa Cruz Biotechnology), antiphosphotyrosine (PY20 mouse monoclonal, Transduction Laboratories, Becton Dickinson, Pont de Claix, France).

Secondary antibody for immunofluorescence were (Jackson Immunoresearch Laboratories, Interchim, Mountlucon, France) fluorescein isothiocyanate-conjugated donkey anti-mouse immunoglobulin G (IgG). Secondary antibodies for western blotting were (GE Healthcare, Orsay, France) horseradish peroxidase (HRP)-conjugated goat anti-mouse IgG and HRP-conjugated goat anti-rabbit IgG.

Affinity-binding assay, immunoprecipitations, SDS–PAGE and immunoblots

Affinity-binding assay using Rhotekin-Rho-binding domain (RBD) or PAK-cdc42/Rac interacting and binding domain (PAK-CRIB) to determine the presence of activated RhoA or Rac1, immunoprecipitations using anti-Vav or anti-Abl, sodium dodecyl sulfate–PAGE (SDS–PAGE), western blots and immunorevelation were performed as previously described (Harnois *et al*., 2003). CGP-571 was provided generously by E Buchdunger (Novartis).

Recombinant proteins

Recombinant proteins were prepared as glutathione *S*-transferase fusion proteins in *Escherichia coli* (BL21 strain), purified using glutathione-sepharose beads (GE Healthcare), eluted with glutathione and used as glutathione *S*-transferase (GST)-fusion proteins. The GST-PAK-CRIB domain and GST-RBD (C21) were obtained as pGEX-2T fusion genes (gift of JG Collard, Netherlands Cancer Institute, Amsterdam, NL) and produced as described (Sander *et al*., 1998).

Transwell experiments

Cell migration was assayed using inserts containing 3D matrigel coated on 8 μm porous filters (BD BioCoat Growth Factor Reduced MATRIGEL Invasion Chamber). A total of 2.5×10^4 cells in 1 ml of RPMI1640 culture medium supplemented with 10% fetal calf serum (FCS) were added to the inserts, while 750 μl of the same culture medium were added in the wells. Cells were incubated for 48 h at 37 °C in a CO_2 incubator. Cells were counted using an ocular micrometer every 24 h. We measured in parallel the proliferation rate during the transwell experiment. Data presented are the result of total migrated cell counting divided by the proliferation rate at the indicated times. Data are presented as relative migration using wild-type Ba/F3 cells as control and represent mean ± s.d. of five or six experiments.

ShRNA transfection and characterization

Sequences of *vav*-specific and control shRNA were contained in pGeneClip hMGFP vector (control shRNA-GGAATCT CATTCGATGCATAC-; shRNA1-AGCCATATGTTCCTT CTGATT- and shRNA2-TGCCCAGAACAAAGGAATCAT-) (SuperArray Bioscience Corporation, Frederick, MD, USA). Plasmids containing control shRNA and *vav*-specific shRNA were produced in *E. coli*. Plasmid maxipreparation were performed using Qiafilter MaxiPrep (Qiagen, Courtaboeuf, France) and DNA concentrations were measured by spectrophotometry. A total of 2 μg of each shRNA was transfected in Ba/F3p190 or Ba/F3p210 cells using a nucleofector device with cell line Nucleofector kit V (Amaxa biosystems, Köln, Germany). Cells were incubated at 37 °C with 5% CO_2 during 24 h, counted and seeded on transwell inserts as described above. A part of the cells was cultured for additional 24 h, counted and lysed as described above for western blot and GST-PAK-CD pull-down analysis. In parallel, FACS analysis of GFP and Vav content of transfected cells was performed on a FACScanto II (Becton-Dickinson).

Time-lapse recordings

A total of 10^5 cells were collected, centrifuged and included in $2\,mg\,ml^{-1}$ liquid Matrigel (Becton Dickinson) or $2\,mg\,ml^{-1}$ Collagen (Becton Dickinson) diluted in RPMI1640 supplemented with 10% FCS at 4 °C. The mixture was then cast into a 1 cm diameter 2 mm high Teflon ring on a 30 mm coverslip. Cells on the coverslip were then incubated for 6 h at 37 °C in a CO_2 incubator. For C3 exoenzyme experiment, cells were preincubated with Ia-C3 ($5\,\mu g\,ml^{-1}$) and Ib ($8\,\mu g\,ml^{-1}$) for 6 h at 37 °C according to Marvaud *et al*. (2002) before inclusion into Matrigel.

Cell imaging with differential interference contrast microscopy was performed by means of an Olympus FV1000 laser scanning confocal station, equipped with a 30 mW multiline argon laser. The confocal unit was connected to an inverted microscope (Olympus IX81, Tokyo, Japan). Maximal resolution was obtained with Olympus Uplan apo × 60 water, 1.3 numerical aperture objective lens. Images were recorded each second for 10 min. Movies presented in Supplementary section were cut to 4 or 5 min and are 12-fold accelerated (12 frames per s).

Statistics

Results are expressed as mean ± s.e.m. of n observations. Sets of data were compared with a Student's t-test. Differences were considered statistically significant when $P<0.05$ (ns, not significant difference; $^{**}P<0.01$; $^{***}P<0.001$). All statistical tests were performed using GraphPad Prism version 4.0 for Windows (Graphpad Software).

Acknowledgements

We are grateful to Dr Michel Popoff (Unité des Toxines Microbiennes, Institut Pasteur, Paris) for providing us with Ia-C3/Ib. Many thanks to Dr Anne Cantereau for helpful and efficient confocal station technical assistance. We also thank Maria Barreira-Gonzalez and Mélanie Magnan for technical assistance, Pr Jean-Marc Gombert and Angélique Chavineau for FACS analysis and Dr Sylvie Chevalier (Inserm U564,

Angers) for providing the Amaxa transfection device. This work was in part supported by grants provided by the 'Ligue Nationale contre le Cancer, Charente-maritime, Charente and Vienne'. Thomas Daubon is recipient of a fellowship from MENRT. This manuscript is dedicated to the memory of Professor Pierre V Vignais.

References

Bassermann F, Jahn T, Miething C, Seipel P, Bai RY, Coutinho S *et al*. (2002). Association of Bcr-Abl with the proto-oncogene Vav is implicated in activation of the Rac-1 pathway. *J Biol Chem* **277**: 12437–12445.

Bhatia R, Munthe HA, Verfaillie CM. (1999). Role of abnormal integrin-cytoskeletal interactions in impaired beta1 integrin function in chronic myelogenous leukemia hematopoietic progenitors. *Exp Hematol* **27**: 1384–1396.

Bustelo XR. (2000). Regulatory and signaling properties of the Vav family. *Mol Cell Biol* **20**: 1461–1477.

Chuang TH, Xu X, Kaartinen V, Heisterkamp N, Groffen J, Bokoch GM. (1995). Abr and Bcr are multifunctional regulators of the Rho GTP-binding protein family. *Proc Natl Acad Sci USA* **92**: 10282–10286.

Clark SS, McLaughlin J, Timmons M, Pendergast AM, Ben-Neriah Y, Dow LW *et al*. (1988). Expression of a distinctive BCR-ABL oncogene in Ph1-positive acute lymphocytic leukemia (ALL). *Science* **239**: 775–777.

Crespo P, Schuebel KE, Ostrom AA, Gutkind JS, Bustelo XR. (1997). Phosphotyrosine-dependent activation of Rac-1 GDP/GTP exchange by the vav proto-oncogene product. *Nature* **385**: 169–172.

Daley GQ, Baltimore D. (1988). Transformation of an interleukin 3-dependent hematopoietic cell line by the chronic myelogenous leukemia-specific P210bcr/abl protein. *Proc Natl Acad Sci USA* **85**: 9312–9316.

Daley GQ, Van Etten RA, Baltimore D. (1990). Induction of chronic myelogenous leukemia in mice by the P210bcr/abl gene of the Philadelphia chromosome. *Science* **247**: 824–830.

Deininger MW, Goldman JM, Melo JV. (2000). The molecular biology of chronic myeloid leukemia. *Blood* **96**: 3343–3356.

Friedl P, Wolf K. (2003). Tumour-cell invasion and migration: diversity and escape mechanisms. *Nat Rev Cancer* **3**: 362–374.

Harnois T, Constantin B, Rioux A, Grenioux E, Kitzis A, Bourmeyster N. (2003). Differential interaction and activation of Rho family GTPases by p210bcr-abl and p190bcr-abl. *Oncogene* **22**: 6445–6454.

Hernandez SE, Krishnaswami M, Miller AL, Koleske AJ. (2004). How do Abl family kinases regulate cell shape and movement? *Trends Cell Biol* **14**: 36–44.

Ilaria Jr RL, Van Etten RA. (1996). p210 and p190(BCR/ABL) induce the tyrosine phosphorylation and DNA binding activity of multiple specific STAT family members. *J Biol Chem* **271**: 31704–31710.

Lugo TG, Pendergast AM, Muller AJ, Witte ON. (1990). Tyrosine kinase activity and transformation potency of bcr-abl oncogene products. *Science* **247**: 1079–1082.

Marvaud JC, Stiles BG, Chenal A, Gillet D, Gibert M, Smith LA *et al*. (2002). *Clostridium perfringens* iota toxin. Mapping of the Ia domain involved in docking with Ib and cellular internalization. *J Biol Chem* **277**: 43659–43666.

Matsuguchi T, Inhorn RC, Carlesso N, Xu G, Druker B, Griffin JD. (1995). Tyrosine phosphorylation of p95Vav in myeloid cells is regulated by GM-CSF, IL-3 and steel factor and is constitutively increased by p210BCR/ABL. *EMBO J* **14**: 257–265.

Nakashima S, Nozawa Y. (1999). Possible role of phospholipase D in cellular differentiation and apoptosis. *Chem Phys Lipids* **98**: 153–164.

Raftopoulou M, Hall A. (2004). Cell migration: Rho GTPases lead the way. *Dev Biol* **265**: 23–32.

Salgia R, Li JL, Ewaniuk DS, Pear W, Pisick E, Burky SA *et al*. (1997). BCR/ABL induces multiple abnormalities of cytoskeletal function. *J Clin Invest* **100**: 46–57.

Sander EE, van Delft S, ten Klooster JP, Reid T, van der Kammen RA, Michiels F *et al*. (1998). Matrix-dependent Tiam1/Rac signaling in epithelial cells promotes either cell-cell adhesion or cell migration and is regulated by phosphatidylinositol 3-kinase. *J Cell Biol* **143**: 1385–1398.

Sawyers CL. (1999). Chronic myeloid leukemia. *N Engl J Med* **340**: 1330–1340.

Stasia MJ, Jouan A, Bourmeyster N, Boquet P, Vignais PV. (1991). ADP-ribosylation of a small size GTP-binding protein in bovine neutrophils by the C3 exoenzyme of *Clostridium botulinum* and effect on the cell motility. *Biochem Biophys Res Commun* **180**: 615–622.

Unwin RD, Sternberg DW, Lu Y, Pierce A, Gilliland DG, Whetton AD. (2005). Global effects of BCR/ABL and TEL/PDGFRbeta expression on the proteome and phosphoproteome: identification of the Rho pathway as a target of BCR/ABL. *J Biol Chem* **280**: 6316–6326.

Van Etten RA. (1999). Cycling, stressed-out and nervous: cellular functions of c-Abl. *Trends Cell Biol* **9**: 179–186.

Wertheim JA, Forsythe K, Druker BJ, Hammer D, Boettiger D, Pear WS. (2002). BCR-ABL-induced adhesion defects are tyrosine kinase-independent. *Blood* **99**: 4122–4130.

Yamazaki D, Kurisu S, Takenawa T. (2005). Regulation of cancer cell motility through actin reorganization. *Cancer Sci* **96**: 379–386.

Zheng J, Chen RH, Corblan-Garcia S, Cahill SM, Bar-Sagi D, Cowburn D. (1997). The solution structure of the pleckstrin homology domain of human SOS1. A possible structural role for the sequential association of diffuse B cell lymphoma and pleckstrin homology domains. *J Biol Chem* **272**: 30340–30344.

Supplementary Information accompanies the paper on the Oncogene website (http://www.nature.com/onc).